CSCE Annual Conference

Growing with youth – Croître avec les jeunes

Laval (Greater Montréal)

June 12 - 15, 2019

IMPLEMENTING UNSUPERVISED MACHINE LEARNING TO GAIN A BETTER UNDERSTANDING OF THE ASPHALT PAVEMENT CONDITIONS OF ONTARIO PROVINCIAL HIGHWAYS

Guangyuan Zhao,[1] Ju Huyan,[1, 3] Susan Tighe,[1] and Wei Li[2]

[1] Centre for Pavement and Transportation Technology, Department of Civil and Environmental Engineering, Faculty of Engineering, University of Waterloo, Canada

[2] School of Information Engineering, Chang'an University, Xi'an, Shaanxi Province, China

[3] jhuyan@uwaterloo.ca

Abstract: Currently, the Ministry of Transportation of Ontario (MTO) obtains its pavement condition data via the Automated Road Analyzer (ARAN), an automated data collection vehicle and system, as part of its pavement management system activities. However, the pavement surface distress types that ARAN is able to discern are limited to cracking only. Without changing the formula used for the Pavement Condition Index, the pavement performance category could be misclassified. In this paper, instead of predicting target performance index values, the authors adopt unsupervised machine learning techniques, i.e., principal component analysis (PCA) and K-means clustering, to understand 2015 MTO asphalt pavement condition data that include 1,410 pavement sections. PCA is conducted to learn about the interrelationships among different key performance indices and employs the clustering method to categorize MTO provincial highways into three performance groups within each road functional class. In summary, this paper outlines an alternative approach to pavement condition assessment and could serve as a reference to facilitate decision-making for highway authorities.

Keywords: Pavement management system (PMS), pavement performance assessment, pavement condition survey, Distress Manifestation Index (DMI), International Roughness Index (IRI), Pavement Condition Index (PCI)

1. BACKGROUND

1.1 Pavement Performance Assessment

Pavement performance assessment plays an important role in both network-level and project-level pavement management systems (PMSs) and provides essential information for highway authority personnel when they make decisions regarding planning, policy, and budget. A comprehensive pavement performance assessment involves a pavement condition survey, ratings, and performance category assignments. Pavement condition surveys are used to collect data related to pavement serviceability and physical conditions. Currently, ASTM D6433 (ASTM 2011) is one of the most widely accepted standards that highway agencies use when collecting surface distress data across North America. FHWA-HRT-13-092 (Miller and Bellinger 2014), proposed by the Federal Highway Administration (FHWA), is another standard practice adopted by several highway agencies and serves also as the guideline for pavement condition evaluation in the Long-Term Pavement Performance program (Hong et al. 2010). The Ministry of Transportation of Ontario (MTO) follows the standard practice, SP-024 (MTO 2016), for surveying and rating

flexible pavement conditions based on distress manifestations, expressed as distress manifestation index (DMI) values. In addition to using the DMI, current MTO practice also considers pavement smoothness (ride quality) as represented by the international roughness index (IRI) as the key performance index (KPI) in the condition rating scheme. To assess overall pavement conditions, the MTO developed a pavement condition index (PCI) formula that incorporates the interrelated DMI and IRI, as shown in Equation 1 (MTO 2009).

[1] $PCI_{MTO} = a + b \times DMI - c \times IRI$

where, *a*, *b*, and *c* are the coefficients and vary for different pavement types. The DMI has a scale of 0 to 10 (most distressed to free of distress) and the IRI is on a scale of 0 to infinity (smooth to rough).

Pavement surface distresses have been rated subjectively for many years based on data that have been collected manually by trained inspectors. However, issues and problems have arisen that are associated with the unreliability and inconsistency of such manually collected data and as a result, researchers have carried out studies to investigate automated pavement surface distress detecting technologies. In particular, such studies have focused on the application of digital image processing-based approaches such as image filtering, image segmentation, feature extraction, and characteristic calculation methodologies (Zuo et al. 2008, Chu et al. 2003, Xu et al. 2008, Zalama et al. 2014, Tsai et al. 2009, Oliveira and Correia 2009). In 2013, in order to improve the accuracy and efficiency of pavement condition assessments as well as to ensure the safety of inspectors, the MTO started transitioning from manual to fully automated data collection for its distress detection and ride quality measurements by utilizing the Automated Road Analyzer (ARAN) (Cafiso et al. 2017, Chan et al. 2016). The ARAN vehicle is equipped with an advanced laser profilometer, a laser crack measurement system, two high-definition cameras, and an accompanying software application for visualizing and processing the pavement imagery and condition data. Calibrated by digital systems for global referencing and positioning, the vehicle is able to operate at various highway speeds, record data continuously, and meanwhile maintain accuracy in terms of location and spatial orientation. In order to distinguish among distress detection, distress reporting, and index computing algorithms used in manual surface distress surveys, ARAN utilizes its own developed PCI formula to represent overall pavement conditions, expressed here as Equation 2.

[2] $PCI_{ARAN} = 0.7 \times IRI_{Scaled} + 0.2 \times DMI_{ARAN} + 0.1 \times RUT_{Scaled}$

where *RUT* is a key performance index that reflects the rutting severity and magnitude in the pavement. $IRI_{Scaled} = 100 \times (1 - IRI/5)$ and $RUT_{Scaled} = 100 * (1 - RUT/30)$.

1.2 Issues

Since 2014, MTO pavement condition data have been collected annually only by ARAN, but the DMI values calculated by ARAN capture only cracking-related distresses; the rating algorithms for other common distresses such as bleeding and raveling are still under development. As a result, DMI_{ARAN} is merely a cracking-based distress performance indicator, and thus, PCI_{ARAN} cannot be compared with PCI_{MTO} directly. Although the MTO has identified the inconsistencies between manually and automatically generated DMI values, the MTO still uses DMI_{ARAN} instead of DMI_{MTO} in Equation 1 to compute the PCI, resulting in questionable PCI values and related performance categories. Because the true PCI-defined performance categories are not known, this paper proposes a data-driven approach that uses unsupervised machine learning techniques to classify pavements into different performance groups. Compared with conventional statistical methods, unsupervised machine learning techniques, such as principal component analysis (PCA) and K-means clustering, offer advantages for handling the interactions among interrelated variables, identifying hidden data structures, and partitioning the data in a more robust and accurate way (Fwa et al. 1997). To apply unsupervised learning techniques to the data in this study, all the analyses are performed using *R*, a statistical computing software application (R Core Team 2018).

2 UNSUPERVISED MACHINE LEARNING TECHNIQUES

2.1 Database and Key Variables

The 2015 asphalt pavement condition data for MTO provincial highways were collected and processed using ARAN 9000 and ARAN 7000. Based on the road functional class, the total numbers of pavement sections for freeways, arterials, collectors, and local roads were 515, 620, 123, and 152, respectively. Although rutting data have been collected by ARAN, a rutting-related index has not been incorporated into calculating the PCI or categorizing pavement conditions. To identify the effects manifested by the rutting data, the 2015 database includes three variables, i.e., the KPIs: DMI, IRI, and *RUT*. The DMI ranges from 0 to 10; higher values represent fewer distresses. By contrast, a higher IRI value indicates a rougher pavement surface, and *RUT* values range from 0 to 30, where higher values indicate more severe rutting. Overall, the DMI has a mean of 8.38 with a standard deviation (SD) of 0.75, the IRI has a mean of 1.34 with a SD of 0.6, and *RUT* has a mean of 3.54 with a SD of 2.12.

Figure 1 presents a chart to aid in visualizing the data. The distribution of each variable can be found in the histograms on the diagonal. The distributions of the IRI and *RUT* values are skewed to the right whereas the distribution of the DMI values is skewed to the left, which implies that highways are generally well maintained. In the lower left part of this figure, scatter plots with fitted lines are displayed for each pair of variables. The scatter plots show seemingly linear relationships among all the variables. The figure's upper right section provides the Pearson correlation coefficient as well as its significance. Clearly, the significant relationship for each pair of variables, represented by the three stars, confirms that the IRI, *RUT*, and DMI are interrelated, and the strength of the relationship between the DMI and *RUT* is the greatest with a correlation coefficient of -0.56.

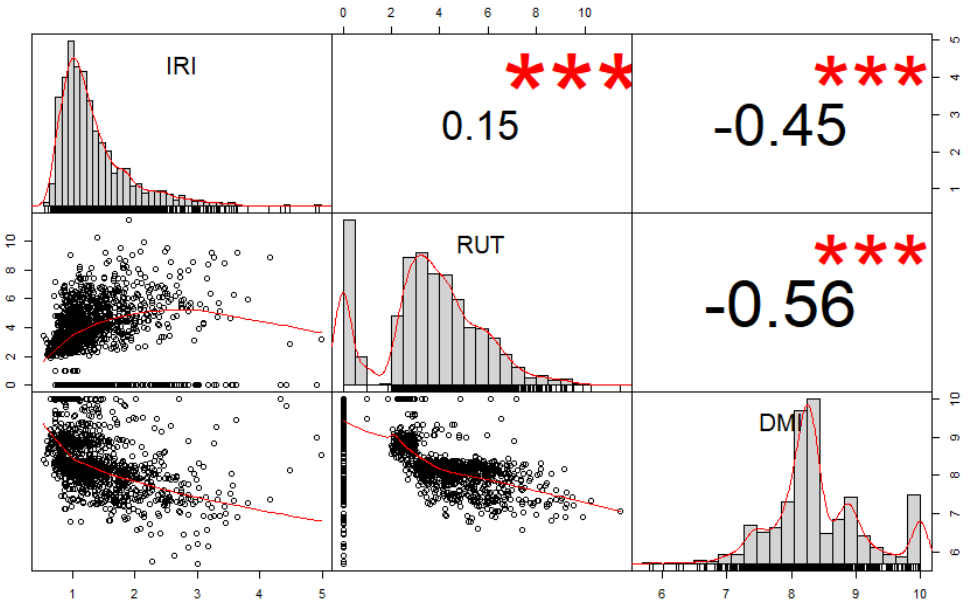

Figure 1 Data distribution and correlation analysis.

2.2 Principal Component Analysis

PCA is a widely used dimensionality reduction technique. By projecting data from the initial space onto the subspace (formed by orthogonal principal components), typically a large set of correlated variables can be reduced to a smaller set that still contains most of the information in the larger set (Bianchini 2013). In this

study, PCA is performed using a covariance matrix $\boldsymbol{\Sigma}$ of existing *p* variables (i.e., the IRI, DMI, and *RUT*), represented by $\boldsymbol{X}' = [X_1, X_2, \dots, X_p]$. The calculated eigenvalue-eigenvector pairs from $\boldsymbol{\Sigma}$ can be expressed as $(\lambda_1, \boldsymbol{e_1}), (\lambda_2, \boldsymbol{e_2}), \dots, (\lambda_p, \boldsymbol{e_p})$, where $\lambda_1 \geq \lambda_2 \geq \cdots \geq \lambda_p \geq 0$, and $\boldsymbol{e_i}$ is the loading vector. As a result, the i^{th} principal component (PC) can be denoted as $Y_i = e_i'\boldsymbol{X} = e_{i1}X_1 + e_{i2}X_2 + \cdots + e_{ip}X_p$ with properties $Var(Y_i) = \boldsymbol{e_i'\Sigma e_i} = \lambda_i$ and $Cov(Y_i, Y_k) = \boldsymbol{e_i'\Sigma e_k} = 0$, where $i = 1,2, \dots, p$ and $i \neq k$. Therefore, the PCs are uncorrelated linear combinations of the existing *p* variables with variances that are equal to the eigenvalues of $\boldsymbol{\Sigma}$. A larger eigenvalue means more information is explained by the PC, so keeping only a few PCs is reasonable because they can explain most of the information. In addition, it should be noted that the magnitude of the variable can greatly impact the PCA results, and the PCs generally place more weight on variables with greater variance. To minimize the effects of the magnitude to certain variables, the IRI, *RUT*, and DMI in this paper were scaled first to have a mean of zero and a standard deviation of one prior to conducting PCA.

Table 1 presents the PCA outputs for each road functional class. In general, the first PC (PC1) explains more than 50% of the total variance. For the collector roadways, the proportion of the total variance that is due to PC1 is as high as 70 percent. For all the road functional classes, the total variance obtained for the first two PCs ranges from 85% to 90%, indicating that PC1 and PC2 can provide a summary of the original data with sufficient accuracy, and PC3 can be dropped in later analysis.

Table 1 Loadings and Total Variance Explained by Principal Components

Functional Class	Variable	PC1	PC2	PC3
Freeway	IRI	-0.517	-0.830	-0.211
	RUT	-0.587	0.523	-0.618
	DMI	0.623	-0.195	-0.757
	Cumulative Proportion of Variance	65.8%	87.9%	100%
Arterial	IRI	-0.519	-0.841	0.154
	RUT	-0.592	0.483	0.645
	DMI	0.617	-0.243	0.749
	Cumulative Proportion of Variance	68.9%	89.4%	100%
Collector	IRI	-0.532	0.810	-0.248
	RUT	-0.580	-0.561	-0.591
	DMI	0.617	0.170	-0.768
	Cumulative Proportion of Variance	70.1%	89.8%	100%
Local	IRI	-0.595	0.531	0.603
	RUT	-0.428	-0.844	0.322
	DMI	0.681	-0.067	0.730
	Cumulative Proportion of Variance	54.5%	85.1%	100%

Figure 2 shows that the PCA results can be illustrated further using biplots. Each PCA biplot includes both a loading plot (axes not shown) and a score plot with PC1 as the horizontal axis and PC2 as the vertical axis. As the PCs are linear combinations of the three variables, PC1 and PC2 are calculated as scores for each observation (pavement section), which are plotted as dots in the figure. The lighter blue dots indicate longer pavement sections and darker blue indicates shorter sections. Consistent with the information shown in Table 1, the loading vector for each variable is depicted as an arrow. Figure 2 also shows that the loading vector for PC1 places approximately equal weight on the IRI, *RUT*, and DMI, whereas the PC2 loading vector puts much less weight on the DMI. For freeways, arterials, and collectors, most weight in PC2 is placed on the IRI, but in comparison, for local roads most weight in PC2 is put on *RUT*. Overall, the loading sign of the DMI is the opposite to that of the IRI and RUT in PC1, which is similar to the form of Equation 1, indicating that PC1 roughly corresponds to the pavement condition expressed by the PCI. The PC2 loading vectors for all the road functional classes indicate that the loading sign of the IRI is always the reverse of that of *RUT*. With limited impact from the DMI (for example, on local roads, the loading of the DMI is as small as -0.067), PC2 is essentially the weighted difference between the IRI and *RUT*. Despite the sample size for each road functional class, more dots are close to the plot origin for the freeways and arterials, which suggests that more pavement sections in freeways and arterials experience average pavement

conditions. By contrast, the dispersed dots indicate that local roads tend to have either 'good' or 'poor' pavement conditions. The effects of pavement section length on pavement conditions are further investigated, but no clear patterns have been found among all the road functional classes.

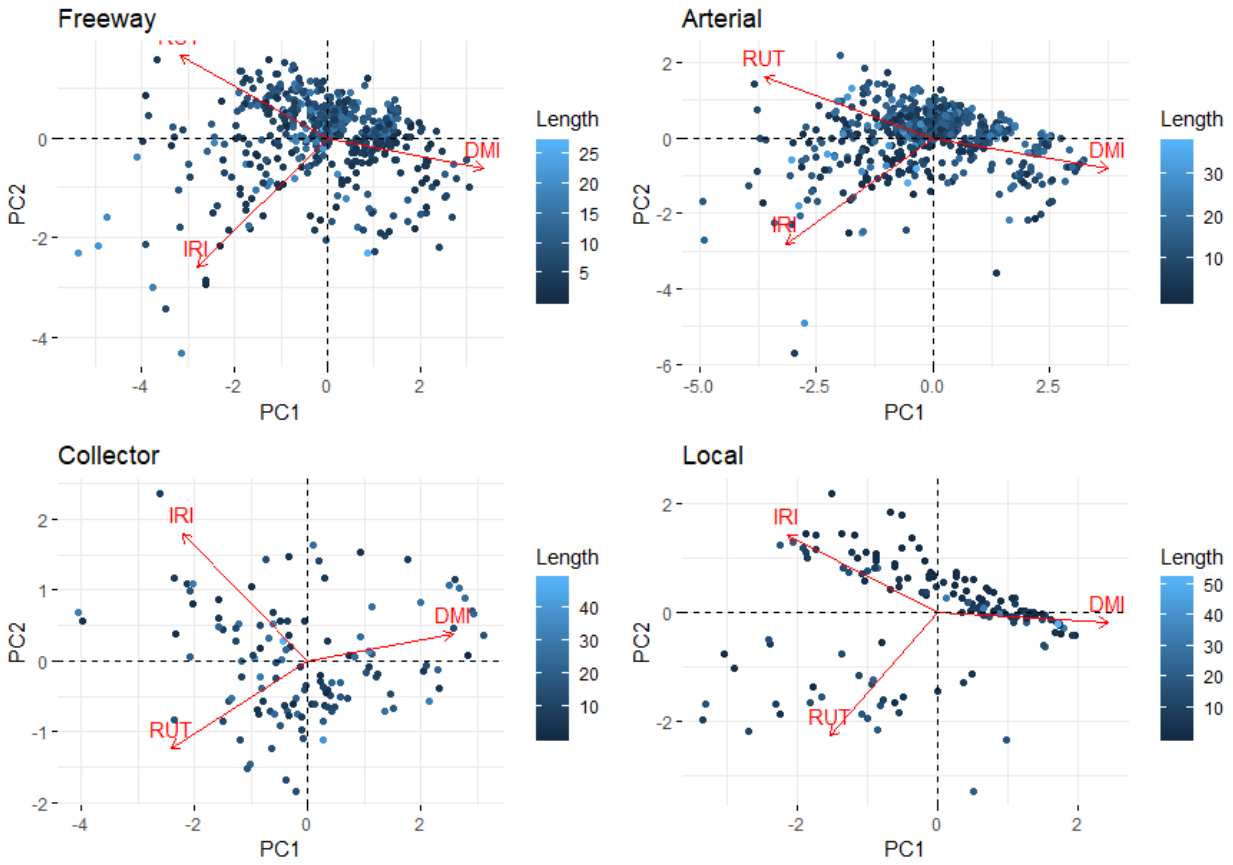

Figure 2 Principal component analysis biplots.

2.3 Clustering – K-means

With the two-dimensional representation of pavement data obtained from PCA in hand, the K-means clustering method is utilized to determine the homogeneous subgroups among all the MTO's provincial pavement sections. According to Li et al. (2015), the procedures of the K-means method can be summarized as follows:

1) Define the *K* clusters.

2) Initially assign a cluster number from 1 to *K* and determine the centroids for all clusters. The k^{th} centroid is the vector of the feature means obtained from PC1 and PC2 for all the observations located in the k^{th} cluster.

3) Iterate the process by moving any observation to the cluster with the smallest Euclidean distance and then update the related centroids until no changes are available in the cluster assignment.

The Elbow method is employed to determine the optimal number of clusters. This method employs the K-means clustering algorithm by varying the *K* value from 1 to 10. Then, the total within-cluster sum of the squares (WSS) is calculated, expressed as $\sum_{k=1}^{K}\sum_{i\in S_k}\sum_{j=1}^{p}(x_{ij}-\bar{x}_{kj})^2$, where S_k is the set of the k^{th} cluster and $\bar{x}_{kj}$ is the k^{th} cluster center by the j^{th} variable. Figure 3 presents the WSS values as a function

of the number of *K* values. The *K* values should be chosen such that adding more clusters does not reduce the WSS significantly. The bend in each plot clearly suggests that the optimal number of *K* is three for all highway functional classes.

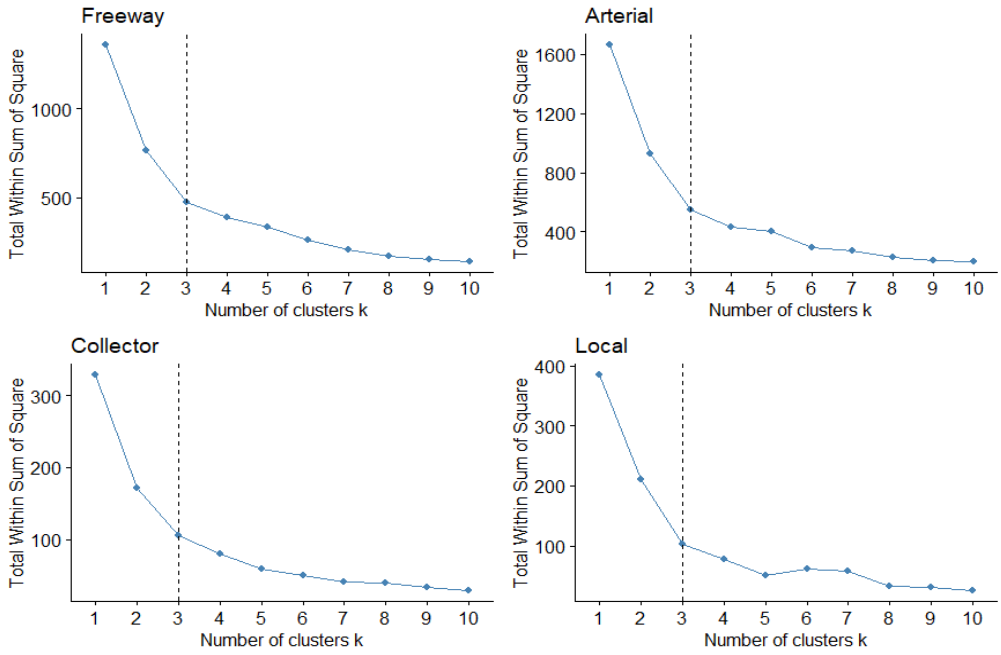

Figure 3 Determination of optimal number of clusters.

By implementing the K-means clustering method, the database is divided into three clusters; Table 2 provides a summary of the means and SDs of the KPIs within each cluster by road functional class.

Table 2 Key Performance Index Values by Cluster and Road Functional Class

		N	IRI		RUT		DMI	
			Mean	SD	Mean	SD	Mean	SD
Freeway	Cluster 1	186	0.95	0.23	2.09	1.08	9.04	0.50
	Cluster 2	264	1.01	0.17	4.35	1.18	8.16	0.25
	Cluster 3	65	1.82	0.41	5.59	1.88	7.66	0.36
Arterial	Cluster 1	157	1.00	0.29	1.71	1.23	9.28	0.55
	Cluster 2	353	1.25	0.27	4.32	1.23	8.16	0.31
	Cluster 3	110	2.26	0.61	6.09	1.75	7.61	0.44
Collector	Cluster 1	31	1.05	0.29	1.53	1.38	9.44	0.62
	Cluster 2	71	1.42	0.34	4.32	1.31	7.98	0.40
	Cluster 3	21	2.52	0.43	5.48	1.58	7.60	0.41
Local	Cluster 1	76	1.34	0.41	0.20	0.77	9.28	0.60
	Cluster 2	27	2.10	0.88	5.20	1.46	7.61	0.63
	Cluster 3	49	2.73	0.69	0.00	0.00	7.73	1.04

For the freeways, arterials, and collectors, Cluster 2 has the largest number of observations followed by Cluster 1 and Cluster 3. For the local roads, on the other hand, the highest proportion of observations is classified into Cluster 1. In general, Cluster 1 is a collection of the pavement sections with the lowest IRI and RUT values but the highest DMI values, whereas Cluster 3 is the opposite. Hence, the K-means clustering method was able to differentiate the database into three groups, where Cluster 1 represents those pavement sections with good pavement conditions, Cluster 2 represents an intermediate level of

pavement conditions, and Cluster 3 represents those pavement sections with relatively poor pavement conditions.

3 DISCUSSION

3.1 Comparisons with Pavement Condition Index

To evaluate the effectiveness of the developed clustering method described in this paper, the PCI values computed from the DMI and IRI are used as the baseline for comparison. Figure 4 presents a boxplot for each road functional class with the PCI as the vertical axis and the cluster group as the horizontal axis. The dashed red lines in the figure are MTO PCI thresholds that are used to define the pavement conditions as 'good', 'fair', or 'poor'. Note that the PCI thresholds vary based on the road functional class. The blue dots are outliers, defined as being away from the 1.5 times interquartile range of the lower and upper quantiles. Generally, for the freeways, arterials, and collectors, Cluster 1 and Cluster 2 fall into the 'good' condition category as defined by the PCI, and Cluster 3 corresponds to the 'fair' condition. The clustering method cannot explicitly discern which cluster indicates 'poor' conditions because the number of 'poor' pavement sections is usually small and the MTO ensures that maintenance activities are undertaken in a timely manner for the 'fair' condition pavements before their conditions turn into 'poor' conditions. Nonetheless, the clustering method developed in this paper still helps to identify variations that are present in pavements with 'good' conditions. The Cluster 2 pavement sections could potentially become candidates for pavement preservation treatments in the following years and thus might be helpful in prioritizing pavement sections for maintenance and managing budgets.

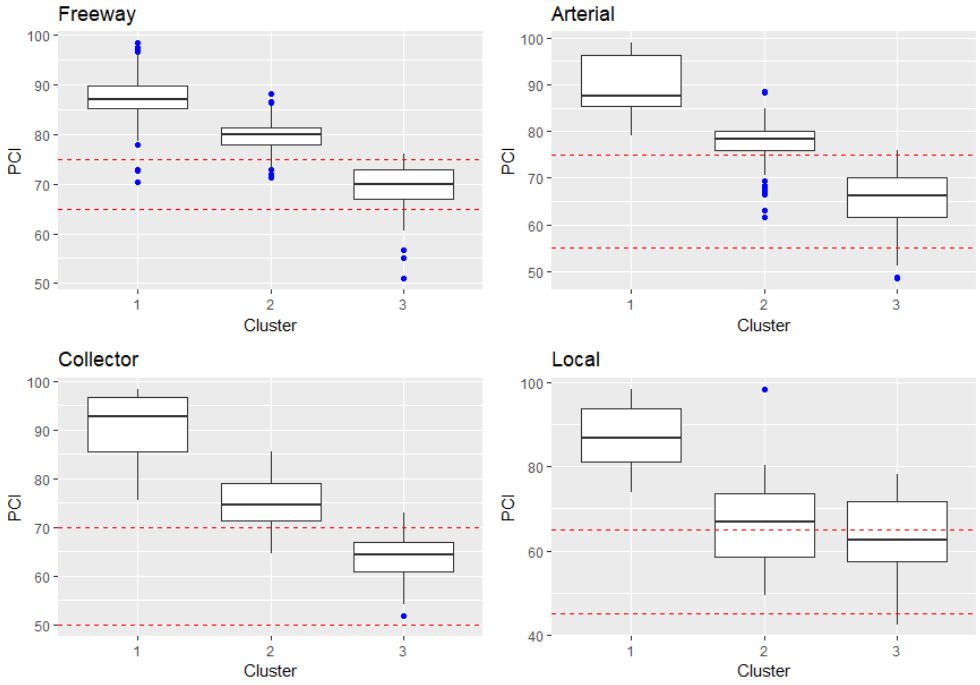

Figure 4 Pavement condition index boxplots by cluster.

3.2 Comparisons with Pavement Performance Category Adjusted by Key Performance Indices

According to the MTO (Li et al. 2011), 'poor' pavement conditions can be triggered by individual KPIs, such as the DMI and IRI. For example, for freeways, 'poor' conditions will be assigned to those pavement sections with DMI values less than 5 or IRI values higher than 3.5. Through this process, the number of 'poor' pavement sections has increased by 53 for freeways, 63 for arterials, and 8 for both collectors and

local roads. The distribution of pavement performance categories adjusted by KPI values within each cluster are investigated as well. Figure 5 shows that almost all the pavement sections in Cluster 1 and most of the pavement sections in Cluster 2 are classified as 'good'. 'Fair' pavement sections can be found in Cluster 2 and Cluster 3, and most 'poor' pavement sections are in Cluster 3. It should be noted that differences are evident in the distribution for local roads compared with the other three roadway types. This finding results from the rutting data; 119 out of 152 pavement sections in local roads have zero *RUT* values, but some of those zeros might be missing values, which could adversely affect the clustering results. This finding also suggests that the database should be examined carefully before using any unsupervised learning techniques.

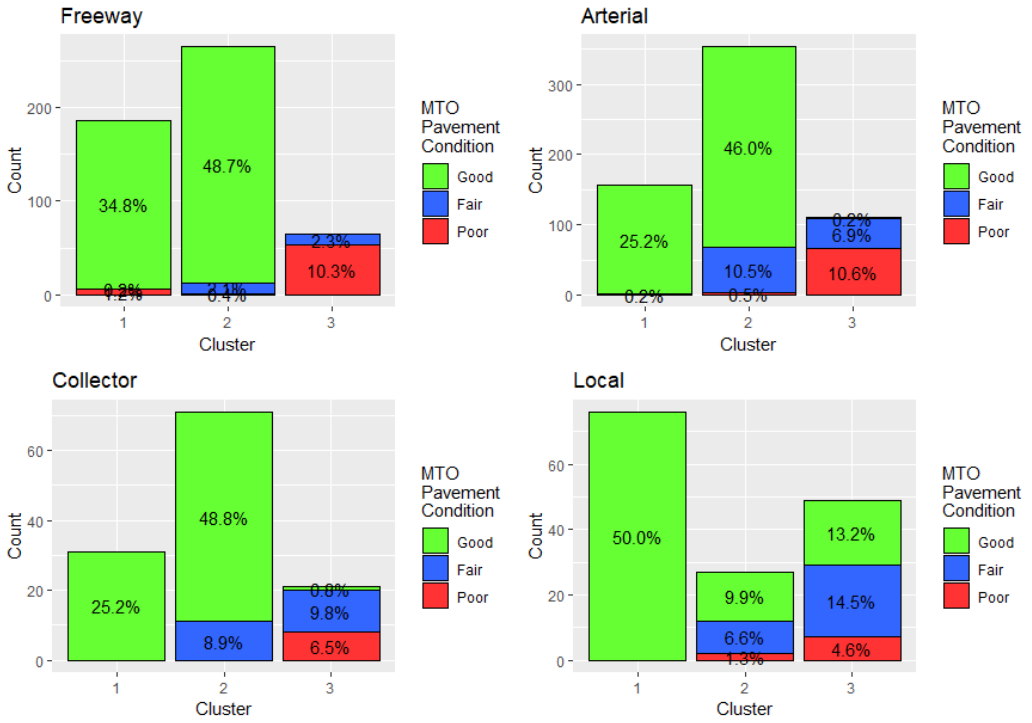

Figure 5 Pavement performance distribution by cluster.

4 SUMMARY AND CONCLUSIONS

Since 2013, a transition from manual to automated pavement condition data collection has taken place for MTO's provincial highways. The use of the newly developed DMI, which considers only cracking-related surface distresses in calculating the PCI, has brought PCI-based performance assessments into question. In this study, asphalt pavement condition data including 1,410 pavement sections, which are automatically collected by ARAN, are analyzed. Three variables are selected that represent various KPIs: the IRI, *RUT*, and DMI. Based on unsupervised machine learning techniques, the following conclusions can be drawn.

- The correlation analysis results show that all the variables are strongly correlated.
- PCA is applied as a dimensionality reduction tool for the exploratory data analysis. The results suggest that PC1 and PC2 can explain more than 85% of the total variance of the data. PC1 has a similar formula as the MTO PCI formula, and PC2 is expressed as the weighted difference between the IRI and *RUT*. Thus, the existing PCI formula does not capture all the data variance and updates for PCI that are needed to consider the PC2 effects. In addition, when KPI values are numerous, PCA proves to be an optimal way to develop an alternative overall pavement condition index using PCs in the form of KPIs.
- Using PC1 and PC2, the K-means clustering method is applied to divide the data into three groups. For

each type of road functional class, it has been found that Cluster 1 represents those pavement sections with the best performance in terms of individual KPIs and Cluster 3 represents those pavement sections with the worst conditions.

- Furthermore, the clustering results are employed to check and compare the distribution of PCI-based performance categories and KPI-adjusted performance categories. The results show that the pavement sections in Cluster 1 and a large proportion of the pavement sections in Cluster 2 are generally in 'good' condition. The pavement sections in Cluster 3 contain almost all the 'poor' condition pavements and some of the 'fair' condition pavements. Hence, this information can be used to improve highway network monitoring and prioritize maintenance activities. The results also suggest that a similar data pattern is present for freeways, arterials, and collectors. The differences found for local roads may be due to missing values in the rutting data.
- The unsupervised machine learning techniques used in the paper can provide valuable insights for 1) better understanding the data, 2) considering multiple KPI effects at the same time, 3) accurately classifying pavements into different groups, and 4) eventually developing alternative performance indices.

5. ACKNOWLEDGEMENTS

The authors would like to thank Dr. Ningyuan Li of the Ministry of Transportation of Ontario for his insightful discussions and suggestions during the research work.

6. REFERENCES

ASTM, D., 2011. 6433-11 Standard Practice for Roads and Parking Lots Pavement Condition Index Surveys. American Society for Testing and Materials. Pennsylvania, USA.

Bianchini, A., 2013. Pavement maintenance planning at the network level with principal component analysis. Journal of Infrastructure Systems, 20(2): 04013013.

Chan, S., Engineer, P.D., Eng, P., Cui, S. and Lee, S., 2016. Transition from Manual to Automated Pavement Distress Data Collection and Performance Modelling in the Pavement Management System. In TAC 2016: Efficient Transportation-Managing the Demand-2016 Conference and Exhibition of the Transportation Association of Canada.

Cafiso, S., D'Agostino, C., Delfino, E. and Montella, A., 2017, June. From manual to automatic pavement distress detection and classification. IEEE In 2017 5th IEEE International Conference on Models and Technologies for Intelligent Transportation Systems (MT-ITS) :433-438.

Chu, J.W., Chu, X.M., Wang, R.B. and Shi, S.M., 2003. Research on Asphalt Pavement Surface Distress Image Feature Extraction Method. Journal of Image and Graphics, 10:1211-1217.

Fwa, T.F., Tan, C.Y. and Chan, W.T., 1997. Backcalculation analysis of pavement-layer moduli using genetic algorithms. Transportation research record, 1570(1):134-142.

Hong, F., Chen, D.H. and Mikhail, M.M., 2010. Long-term performance evaluation of recycled asphalt pavement results from Texas: Pavement studies category 5 sections from the long-term pavement performance program. Transportation Research Record, 2180(1):58-66.

Li, N.Y., Kazmierowski, T. and Koo, A., 2011. Key Pavement Performance Indicators and Prediction Models Applied in a Canadian PMS. In Eighth International Conference on Managing Pavement AssetsFugroFederal Highway AdministrationIntervial ChileCAF-Banco de Desarrollo de America Latina (No. ICMPA064).

Li, Q.J., Wang, K.C., Qiu, S., Zhang, Z.D. and Moravec, M., 2015. Development of simplified traffic loading for secondary road pavement design. International Journal of Pavement Engineering, 16(2):97-104.

Miller, John S, and William Y Bellinger. 2014. Distress identification manual for the long-term pavement performance program. United States. Federal Highway Administration. Office of Infrastructure.

MTO. 2016. "SP-024 Manual for Condition Rating of Flexible Pavements, Distress Manifestations." Ministry of Transportation, Ontario. ISBN 978-1-4606-8020-9.

MTO. 2009. "The Formulations to Calculate Pavement Condition Indices." Ministry of Transportation, Ontario.

Oliveira, H. and Correia, P.L., 2009, August. Automatic road crack segmentation using entropy and image

dynamic thresholding. IEEE.In 2009 17th European Signal Processing Conference: 622-626.
R Core Team (2018). R: A language and environment for statistical computing. R Foundation for Statistical Computing, Vienna, Austria. URL https://www.R-project.org/.
Team, RDC. 2008. "R: A language and environment for statistical computing." R foundation for statistical computing, Vienna, Austria.
Tsai, Y.C., Kaul, V. and Mersereau, R.M., 2009. Critical assessment of pavement distress segmentation methods. Journal of transportation engineering, 136(1):11-19.
Xu, G., Ma, J., Liu, F. and Niu, X., 2008, December. Automatic recognition of pavement surface crack based on BP neural network. IEEE.In 2008 International Conference on Computer and Electrical Engineering :19-22.
Zalama, E., Gómez‐García‐Bermejo, J., Medina, R. and Llamas, J., 2014. Road crack detection using visual features extracted by Gabor filters. Computer‐Aided Civil and Infrastructure Engineering, 29(5):342-358.
Zuo, Y., Wang, G. and Zuo, C., 2008, December. Wavelet packet denoising for pavement surface cracks detection. IEEE.In 2008 International Conference on Computational Intelligence and Security 2:481-484.